HP-LT rocks exhumed during intra-oceanic subduction: the example of the Escambray massif (Cuba).

Julie Schneider, Delphine Bosch, Patrick Monié, Stéphane Guillot, Jean-Marc Lardeaux, Antonio Garcia-Casco, R.L. Torres-Roldan, G.M. Trujillo

HP/LT Rocks Exhumed During Intra-Oceanic Subduction: The Example of the Escambray Massif (Central Cuba)

Julie Schneider[(1)*], Delphine Bosch[(1)], Patrick Monié[(2)], Stéphane Guillot[(3)], Jean-Marc Lardeaux[(3)], Antonio García-Casco[(4)], Rafael Luís Torres-Roldán[(4)] and Guillermo Millán Trujillo[(5)].

[(1)] Laboratoire de Tectonophysique, CNRS UMR 5568, Université Montpellier II, Place E. Bataillon, 34095 Montpellier Cédex, France.

[(2)] Laboratoire de Géophysique, Tectonique et de Sédimentologie, CNRS UMR 5573, Université Montpellier II, Place E. Bataillon, 34095 Montpellier Cédex, France.

(3)Laboratoire de Dynamique de la Lithosphère - CNRS UMR 5570, Université Lyon I et ENS-Lyon, bât Géode, 27 bd du 11 Novembre, 69622 Villeurbanne, France.

[(4)] Dpto. De mineralogía y Petrología, Universidad de Granada, Fuentenueva s/n, 18002-Granada, Spain.

[(5)] Instituto de Geología y Paleontologia, Via Blanca y Carretera Centra, La Habana, Cuba.

* corresponding author : Email : schnei@dstu.univ-montp2.fr

Abstract

High-Presssure metabasites embedded in a serpentinite or metasedimentary matrix from the Sancti Spiritus dome (Escambray massif, Central Cuba) have been studied in order to better understand the origine and the evolution of the Northern Carribean boundary plate during the Cretaceous, in a global subduction context. Geochemical analyses (major, trace elements and isotopes) of the high pressure rocks show that they could be partially derived from the Cretaceous calc-alkaline arc described in Central Cuba, these were probably incorporated in the subduction zone by tectonic erosion. The High-Pressure rocks record a prograde path from the epidote bearing amphibolite facies to the barroisite bearing eclogite facies (P = 19 ± 2 Kbar, T = 590 ± 90 °C). These metabasites show evidence of retrogression starting from the glaucophane bearing eclogite facies to the lawsonite bearing blueschist facies. Therefore, these HP/LT rocks are characterized by a counter-clockwise cooling P/T path, which can be explained by the exhumation of HP rocks while the subduction was still active. Concordant geochronological data (Rb/Sr and Ar/Ar) suggest that the main exhumation of HP/LT rocks from the Sancti Spiritus dome occurred 70 Ma ago by top to SW thrusting. The retrogressed trajectory of these rocks, means that the northeast subduction of the Farallon plate continued after 70Ma. The final exhumation can be correlated with the beginning of the collision between the Bahamas platform and the Cretaceous island arc that induced a change of the subduction kinematic.

Keywords: HP/LT rocks, subduction, exhumation , accretionary wedge, Cuba.

Introduction

Because of our incomplete knowledge about the dynamic, chemical and isotopic processes operating during exhumation of high-pressure (HP) rocks, the mechanisms by which high to ultra high-pressure metamorphic rocks are brought up to the Earth surface are still a matter of debate (e.g. Ernst & Liou, 1999). In most cases, high pressure rock exhumation is generally modelled in continental collision zones, such as the Caledonides, the Himalaya, the Alps and the Dabie Shan, emphasises the role of buoyancy and boundary strengths as driving forces of this process (Anhert, 1970; England & Holland, 1979; Davies & Von Blackenburg, 1995; Chemenda et al., 1995). Because of the importance of late collisional events in most orogenic belts, rarely informations relevant to the early exhumation stages can be obtained. However, in some active subduction zones where evidence of continental collision is lacking (e.g. Marianne Trench, New Guinea, Northern Caribbean), the exposure of large amounts of blueschists and eclogites suggests that exhumation of deeply subducted rocks can occur before collision. The occurrence of high pressure rocks in such an environment implies that the exhumation processes of high pressure rocks during the early stages of convergence are related to the subduction dynamics (Platt, 1986; Allemand & Lardeaux, 1997).

In such a context, the study of the North-Caribbean margin is particularly interesting (Fig. 1a). HP rocks associated with a relatively well preserved paleo-subduction zone are described in several places such as Cuba which has not been affected by the large scale active E-W shearing present along of the northern and southern Caribbean plate boundaries. In the central part of Cuba, HP/LT rocks cropout in the Escambray massif (Southwestern Cuban terranes Fig. 2). Eclogites form metre to hectometre boudins packed in serpentinite or intercalated with

metasediments. The eclogites were formed probably during the Cretaceous convergence between the Farallon plate and the Atlantic plate (Kerr et al., 1999), but there is no consensus about the Mesozoic tectonic scenario for the Caribbean plate.

According to Ernst (1988) and many others, the precise reconstruction of P-T-t path in HP rocks provides constraints on the exhumation context. In order to define the possible mechanisms responsible for HP rock exhumation during active subduction, this paper presents new petrological, geochemical and geochronological data on the HP/LT rocks from the Escambray massif (central Cuba).

Geological setting

The Island of Cuba is a part of the northern segment of the Greater Antilles volcanic arc, which fringes the Caribbean boundary plate and results from the collision between the Cretaceous island arc and the Bahamas platform in the Late Paleocene to the Early Eocene time (Burke, 1988 ; Pindell, 1993; Mann et al., 1995; Iturralde-Vinent, 1996a ; Huston et al., 1998). Since the Paleocene-Early Eocene, Cuba has been isolated from the Caribbean plate by a sinistral strike-slip fault related to the opening of the oceanic Cayman ridge (Wadge & Burke, 1983; Mann et al., 1995; Gorndon & Mann, l997) (Fig. 1a).

According to current models of tectonic evolution of the Caribbean, the Cretaceous island arc was originally built during the subduction of the Farallon plate, beneath the North American plate (Fig. 1b). The development of an oceanic plateau in front of the Pacific subduction zone at the latitude of Central America between the Cenomanian and the Turonian (Kerr et al., l997; Sinton et al, l998) induced a change of the subduction velocity accommodated by the onset of two strike-slip fault systems. Progressively, the incorporation of continental sediments in the subduction

trench due to the progression of the Cretaceous island arc between the North and South American plates induced a change in the island arc magmatism from tholeiitic to calc-alkaline (Kerr et al., 1999) (Fig. 1c). Around Cenomanian time the north-western part of the Cretaceous island arc collided with the Yucatan peninsula (Iturralde, 1996a; Iturralde et al., 1996; Gordon et al., 1997; Grafe et al., 2001, García-Casco et al., 2001) which resulted in the end of the arc magmatic activity and in a change in the subduction regime in this area (Fig. 1d). Eastwards, the Cretaceous magmatism was still active till the Turonian (Iturralde-Vinent, 1996b, 1996c). At the end of the Cretaceous, the subduction polarity at the front of the north-eastern part of the plateau reversed and the subduction of the Atlantic plate started beneath the proto Caribbean plate .

A consequence of the collision of the western segment of the Cretaceous island arc with the Yucatan peninsula and of the approach of the collision between the Bahamas platform and the Greater Antilles arc is the rotation of the north strike slip-fault system from Northeast to East. This involved the progressive accretion of the northern part of the Yucatan basin and of the western and central Cuba to the North American plate from the Paleocene to the Mid-Eocene (Bralower & Iturralde-Vinent, l997; Gorbon & Mann, 1997; Huston et al., 1998). This was followed by the accretion of southern part of Cuba and Hispaniola during the Mid to Late-Eocene (Gordon & Mann, 1997; Huston et al., 1998), and finally of Puerto Ricco during the Oligocene (Dolan et al., 1991) (Fig. 1e).

Thus, Cuba appears as a serie of post-Jurassic accreted terranes of both continental and oceanic affinities (Iturralde-Vinent, l994) (Fig. 2a). Western Cuba is essentially composed of Jurassic sediments correlable with Jurassic continental beds of Central America and Jurassic sediments from the gulf of Mexico. Eastern Cuba represents an upflited part of the Cayman rise (Perfit & Heezen, 1978). This paper focuses on the central part of Cuba (Fig. 2b). Which can be divided into two main units: autochthonous units that are part of the Bahamas platform to the

North, and allochthonous terranes belonging to the Caribbean plate to the South. Autochthonous terranes are composed of folded Jurassic to Cretaceous sediments (Fold Belt) and Paleocene-Eocene foreland basin sediments. To the North, allochthonous terranes consist of an ophiolitic melange (Zaza zone) with remains of the Cretaceous island arc and associated back-arc basin (Kerr & al., 1999) that thrusts onto the autochthonous fold belt. Eclogitic lenses occur here as boudins in a melange made of serpentinite (Somin & Millán, 1981; Millán, 1996a; García-Casco et al., 2002).

The Cretaceous island arc in the central part thrusts the ophiolitic melange up to the north. The southern part is composed of Jurassic to Cretaceous sedimentary rocks of continental margin type, along with some ophiolites and Cretaceous volcanic arc suites outcrop (Somin & Millan, l98l, Blein et al., 2003). This southern unit is divided in two massifs, the Mabujina and the Escambray massifs separated by a sinistral strike slip fault. The Mabujina amphibolitic unit is interpreted as the basement of the Late Cretaceous island arc (Somin & Millan, 1981; Millán, 1996b) and could represent an older Pacific arc accreted to the Early Cretaceous Carribean arc (Blein et al., 2003) . Ar-Ar and Rb-Sr dating of granodiorites and pegmatites cross-cutting the massif yielded ages between 90 and 75 Ma (Graffe et al., 2001) which have been previously interpreted as collision ages between the Cretaceous island arc and the Yucatan peninsula.

The Escambray massif, one of the three metamorphic complexes of the southwestern Cuban terranes, is compose of two metamorphic domes (Fig. 2c): the Trinidad and the Sancti Spiritus domes separated by a Paleogene sedimentary cover (Somin & Millan, 1981; Millan & Somin, 1981, 1985, Millán, 1997b) (Fig. 1b). The Escambray massif is mainly composed of siliciclastic metasediments and subordinate marbles, metabasic rocks and serpentinites. Paleontological evidences (Millan & Somin, 1985) reveals that the metasediments are Jurassic to Cretaceous in age and can divided into three units. Unit I is the lower structural unit and is composed of greenschist facies rocks of pelitic and carbonate composition which record metamorphic

conditions below 500°C for 7-8kbar (Grevel, 2000). Unit II is characterised by basic to ultrabasic boudins showing a lawsonite blueschist metamorphic overprint. Eclogitic lenses preserved in a serpentinite or metasedimentary matrix compose the uppermost unit III. Peak metamorphic conditions for this unit are estimated at 530°C-630°C for a pressure of 16 to 25 kbar (Grevel, 2000). Structural and cartographic evidence (Fig. 2b-c) shows that unit I is pluri-kilometer thick whereas units II and III are very thin (± 1 km). They form a nappe pile associated with early top to the WSW or SW thrusting structures (Millan, 1989 and pers. obs.) underlined by eclogitic minerals (garnet-omphacite-rutile) in unit III, blueschist minerals (glaucophane-lawsonite) in unit II and greenschist minerals (chlorite-epidote) in unit I. Late extensional tectonics, top to the SE developed from blueschist facies to brittle conditions are responsible for the opening of a continental basin during the Paleocene. This latter was infilled by sediments and debris derived from the exhumed eclogites and blueschists during the Eocene (Millan and Somin, 1981).

Previous geochronological studies on the Escambray massif yield ages between 68 and 85 Ma (K-Ar dating on white micas, Somin & Millan, l981; Millan & Somin, 1985; Hatten et al., 1988; Iturralde-Vinent et al., 1996) and around l00 Ma for U-Pb dating on zircon (Hatten et al., l988; 1989). The100 Ma old ages are interpreted as the age of the HP metamorphism, while upper Cretaceous ages are interpreted as exhumation ages. In order to better constrain the timing of exhumation of the Escambray massif, three unweathered samples (LV66, LV69, and CUl6) were selected for petrological study, Rb/Sr and Ar/Ar geochronology. LV69 was collected from eclogitic lenses packed in serpentinites from the Sancti Spiritus dome and LV66 and CU16 were collected from an intercalation within the metasediments of Loma la Gloria formation, which is correlated with Jurassic sediments from Guaniguanico (Millán, 1997a). (Fig. 2b-c)

Analytical Procedures

Mineralogical analyses procedures and calculation methods :

Mineral analyses were performed at the Université Montpellier II on a microprobe CAMECA SX100. Analytical conditions were a 20kV accelerating voltage and 10nA beam current.(rajouter les standards etc..) Fe^{3+} in garnet, omphacite, amphibole, and epidote was recalculated after normalisation to 12 oxygens and 8 cations, 6 oxygens and 4 cations (Morimoto et al., 1988), 23 oxygens and 13 cations (Leake et al., 1997), and 12,5 oxygens and 8 cations ($Fe_{total}=Fe^{3+}$), respectively (report in table 1). Temperature estimates were obtained using garnet-cpx Fe-Mg exchange geothermometers (Ellis & Green, 1979; Powell, 1985; Krogh, 2000) (table x) and garnet-amphibole Fe-Mg exchange geothermometers (Graham & Powell, 1984; Krogh, 2000) (table x). The Graham and Powell thermometer was applied assuming that the Fe_{tot} is reduced (Fe^{2+}) as suggested by the authors. Pressure estimates were obtained by using the garnet-omphacite-phengite geobarometer (Waters & Martin, 1993; see also Carswell et al., 1997, O'Brien et al., 2001). Activiy models correspond to those of Hodges & Spear (1982) for garnet, Holland & Powell (1990) for omphacite, and ideal activity for phengite (table x). All the uncertainties are quoted at the 2σ level.

Geochemical analyses procedures :

Whole rock major element analyses were performed at the CRPG of Nancy (Table 2). Trace and REE element determinations on Whole rocks and mineral fractions were performed by ICP-MS at the Université Montpellier II by using acid dilution of 20 mg samples (rajouter les standards). Rb and Sr concentrations were obtained by isotopic dilution (Table 2). Mineral fractions were obtained after crushing and sieving (100-125µm size fractions) of samples, separation using Frantz isodynamic separator, heavy liquids and finally handpicking. The optical study of inclusions in garnet reveals abundance of clinozoïsite, apatite and rutile, while a SEM study indicated the occurence of minute

zircon inclusions. In order to reduce or eliminate the disturbing effects associated with these inclusions on the $^{143}Nd/^{144}Nd$ ratio, a serie of leaching experiments was performed on garnet fractions, following the procedure described by Zhou & Hensen (1995). Separated minerals were first washed with acetone, and then with distilled water before to being ground in an agate mortar. At this stage, the mineral fractions were leached into hydro-chloric acid (2.5N) to remove surface impurities and alteration traces before to be weighed. Garnets were leached in a 2:HNO_3 (13N) / 1:HCl (6N) solution at 120°C for 2 days. This leaching was done in order to remove phosphate inclusions (monazite or apatite). Solutions were then centrifuged to remove leachates. Solid residuals were rinsed three times with distilled water before weighing. After this stage, the weight difference was important, up to 50% for some garnets. As the silicate phases cannot be dissolved in an HCl/HNO_3 environment, the weight loss is attributed to dissolution of the non-silicate phases. Garnets were oxidised in concentrated HNO_3 at 180°C overnight to make the digestion easier. Finally garnets were digested over pressure in Teflon® bombs in a 2:HF (48%) / 1:HNO3 (13N) mixture at 180°C for three days. The other mineral phases were digested in Savilex® beakers with the same mixture for two days at 120°C. After dissolution, all mineral fractions were evaporated and then put in a HCl 6N solution for several hours in order to complex the REE. After a last centrifugation to eliminate the undigested solid residue (zircon and rutile for instance), and amorphous silica, a fraction of each solutions was recover and spiked for Rb and Sr concentrations calculations. Finally all solutions were evaporated again, and then dilute HCl was added before introduction on ion exchange resin (AGW1X12). Separations were carried out following the procedure described by Birck & Allègre (1978). $^{87}Sr/^{86}Sr$ ratios were measured on a VG sector mass spectrometer at the Université of Montpellier II, $^{87}Sr/^{86}Sr$ ratios of standard NBS 987 were at 0.710245+/-0.0000015. $^{143}Nd/^{144}Nd$ ratios were measured on a Finnigan MAT spectrometer at the Université Paul Sabatier of Toulouse, $^{143}Nd/^{144}Nd$ ratios of standard Renne were at 0.511987+/-0.000006. As we don't know the age of the protolith, corrections for the $^{87}Sr/^{86}Sr$ and $^{143}Nd/^{144}Nd$ initial ratios were carried with the age of the regional metamorphism (70 Ma, see Geochronological section) (Table 3). Isochrons were calculated using the ISOPLOT program (Ludwig, 1994) (Fig. 9).

Ar/Ar dating procedure :

After crushing, 1000-500 μm size fractions were recovered and micas and amphiboles were hand-picked under a binocular microscope for Argon analyses. After acetone, alcohol and distilled water washing, single grains were irradiated in the Mc Master nuclear centre (Canada) together with several MMHb monitor grains (Samson and Alexander, 1987). Single crystals were degassed with a laser-probe using two procedures, step heating and spot

ablation at the Université of Montpellier II. The analytical device is similar to that described by Dalrymple (1989) and consists of a continuous 6W argon-ion laser equipped with a programmable beam shutter, optics for laser beam focusing, a CCD camera used to monitor the experiments, a 300cc extraction-cleanup line and a MAP 215-250 mass spectrometer with a Nier ion source and Johnston MM1 electron multiplier (Monié et al., 1994). Minerals were placed in drilled cores made on a copper plate and heated with a focused or defocused laser beam depending on the procedure chosen for degassing. For step heating experiments, minerals were exposed to the laser beam during 30s for each step. Spot ablation was achieved using an exposure time of 30ms for each spot on the beam shutter. Each age determination requires approximately 20 min for lasering, gas cleaning and data acquisition. Blanks were monitored every two or three experiments, and were about 3.10^{-12} CC and 6.10^{-14} CC for masses 40 to 36 respectively. For each analysis, classical isotope corrections including blanks, mass discrimination, radioactive decay of ^{37}Ar and ^{39}Ar and irradiation-induced mass interferences were applied. The quoted errors represent 1σ deviation and were calculated after MacDougall and Harrisson (1988). Isochron ages were calculated following the regression technique of York (1969) (Fig. 10, Table 4). Generally, the low-temperature heating steps exhibit scatter on isochron diagrams and have been excluded from the regression.

Petrology

Metabasites LV66, LV69 and CU16 contain the assemblage garnet (grt) + amphibole (am) + clinopyroxene (cpx) + white mica + epidote (ep) +/- quartz (qtz) +/- rutile (rt) +/- calcite. Mineral abbreviations used in the text are after Kretz (1983). All samples show a foliation defined by the preferential orientation of micas, cpx and am.

Garnet:

In eclogite LV66 garnet occurs as i) large porphyroblasts (l-0.5 mm) with inclusion-rich cores (core 1) (inclusions of qtz, rt, ap, and graphite) surrounded by inclusion-poor rims (rim 1), and ii) inclusion-poor small neoblasts (100- l 25 μm).

These garnets are in textural equilibrium with clinopyroxene, epidote and mica. The large garnet porphyroblasts are almandine-rich and strongly zoned (Fig. 4a, Table 1). Inclusion-rich cores

(core 1) are characterized by a decrease of the $Mg/(Mg^{2+}+Fe^{2+})$ ratio from 0.2 to 0.09, and an increase in grossular content from 17 to 32%. The $Mg/(Mg^{2+}+Fe^{2+})$ ratio of garnet rims (rim l) rises from 0.09 to 0.3, which is indicative of prograde growth zoning (Alm_{56} Prp_{5} Grs_{32} Sps_{7} to Alm_{54} Prp_{22} Grs_{23} Sps_{2}). Small garnet is compositionally similar to rim l (Alm_{56} Prp_{18} Grs_{25} Sps_{1}).

In CUl6, the eclogitic minerals (garnet and clinopyroxene) are fractured and show significant signs of retrogression. Garnet (l-3 mm) does not show any euhedral boundary, excepted in some contacts with clinopyroxene (Fig. 3c). Small garnets (l00 μm) are also present in the matrix, and appear to be in equilibrium with the blueschist assemblage (glaucophane, paragonite and clinozoïsite). CU16 garnets show complex zonation with three distinct parts (Fig. 4b, Table 1). The inner cores (core 2a) is almandine-rich and grossular-poor (Alm_{62} Prp_{17} Grs_{17} Sps_{4}), and is surrounded by an outer cores (core 2b) marked by a sharp decrease in Fe content, an increase in grossular content (Alm_{57} Prp_{8} Grs_{33} Sps_{2}), and a strong decrease in $Mg/(Mg^{2+}+Fe^{2+})$ ratio from 0.2l to 0.l3. This zonation is similar to that described for the LV66 core l. Finally the $Mg/(Mg^{2+}+Fe^{2+})$ ratio rises rimward (rim2) to 0.2 (Alm_{56} Prp_{15} Grs_{27} Sps_{2}), tracing a prograde growth similar to the LV66 and LV69 garnet. However the final $Mg/(Mg^{2+}+Fe^{2+})$ ratio of CUl6 is lower than the 0.3 ratio measured in LV66. The small garnets present in the matrix have a similar composition to those of the resorbed rim 2. Eclogitic garnet from CU16 shows similar zoning to that in LV66, but their reequilibration in the blueschist facies is much more significant. Their rims have been resorbed since their composition ($Mg/(Mg^{2+}+Fe^{2+})$ of 0.2) equilibrated with the blueschist paragenesis**.(8??)**

In LV69, garnet is generally euhedral and often rimed by chlorite. However some unaltered rims preserve the Grt- Cpx- Am- mica textural relations. Garnet cores are rich in qtz, rt, ap, gr, ep and blue-green amphibole inclusions which define a previous foliation (Fig.3b). Cores of LV69 inclusion-rich garnet (core 3) show a plateau-like pattern around Alm_{56} Prp_{13} Grs_{30} Sps_{2} (Fig.

4c, Table 1). Rimward (rim 3) the $Mg/(Mg^{2+}+Fe^{2+})$ ratio increases sharply from 0.2 to 0.3 while grossular content decreases from 30 to 23% (Alm_{53} Prp_{23} Grs_{23} Sps_{1}). This prograde profile is similar to that described for the LV66 rim l and CU16 rim2. The decrease in the $Mg/(Mg^{2+}+Fe^{2+})$ ratio at the cores of LV66 and CU16 seems to represent a pre-eclogitic-peak retrogressed feature (comprends pas ??). The lack of this feature in LV69 may be related to contrasting geological settings, and may to indicate different pre-subduction histories. **(8 ??)**

Clinopyroxenes:

Clinopyroxene chemical composition of the three analysed samples fall in the range of omphacite (Jadeite between 40 and 45%, (Table 1) according to the Morimoto (l988) classification. No zonation ??

Micas:

Representative mica analyses are reported in Table 1. In LV66, mica consists mainly of paragonite ($Na^{+} \approx 0.4$-0.7. and $Si^{4+} \approx 3$ per 11 oxygen). Phengite occurs in the contact zone with garnet and in the matrix ($K^{+} \approx 0.9$ and $Si^{4+} \approx 3.4$ per 11 oxygens). In CU l6, mica is an abundant phase in the matrix and occurrs as fine flakes of paragonite ($Si^{4+} \approx 2.97$ and $Na^{+} \approx 0.85$ per 11 oxygen). Paragonite inclusions in omphacite have the same chemical composition. Microprobe analysis show the appearance of albite in the paragonite-clinozoïsite contact, corresponding to the following low temperature reaction: Clinozoïsite + paragonite = albite**.(8), (9)** Micas are relatively large up to l mm long in eclogite LV69, only phengite were observed ($Si^{4+} \approx 3.27$ and $K^{+} \approx 0.88$ per 11 oxygens).

Amphiboles:

In eclogite LV66 amphiboles are aligned in the foliation or cross-cuting it . They are often developed around clinopyroxenes. Some of them are optically zoned suggesting the possible

occurrence of inherited cores (Fig. 3a), both core and rim compositions were determined. Core composition falls in the field of barroisite (sodic-calcic amphiboles) whereas rim composition falls in the glaucophane field (Table 1, leake (1997)). According to textural criteria, barroisite is interpreted to have grown during the eclogitic stage, whereas glaucophane is attributed to a retrogressed stage under blueschist facies conditions.

Only glaucophane is observed in CU16 (Fig. 3c, Table 1). This glaucophane forms large patches closely associated with paragonite and including skeletons of garnet and omphacite.

Two generations of amphibole have been distinguished in sample LV69, both on textural and chemical grounds (Fig. 3b, Table 1). Barroisite belongs typically to the eclogitic paragenesis and is mainly present in the matrix. At some contact zones with garnet, glaucophane has been observed, attesting to a partial blueschist facies overprint.

Epidotes:

Two types of epidote have been optically recognised: zoïsite and clinozoïsite. Both are found in the matrix and as inclusions in garnet for the LV69 and LV66 eclogites. Only clinozoïsite was found in CU16. Chemical analyses do not show any significant differences between these two epidotes ($Fe^{3+}/(Fe^{3+}+Al)$ = 0.14-0.16) (Table 1).

Paragenetic evolution:

According to the textural relationships between the minerals described above, three successive metamorphic stages are recognized in the studied metabasites:

Eclogitic stage: garnet + barroisite + omphacite + phengite + zoïsite + rutile +/- quartz.

Blueschist stage: garnet + glaucophane + paragonite + clinozoïsite +/- quartz +/- titanite (destabilisation of rutile).

Thermobarometric estimates of the eclogitic grade:

LV66: Garnet - clinopyroxene thermometry for twelve mineral pairs gives 615 ± 80°C at 20 kbar. This temperature is relatively poorly constrained **(12),** probably because Fe-Mg equilibrium between garnet and clinopyroxene is rarely preserved. These temperatures plot outside the glaucophane stability field (Maresh, 1977**),** which is consistent with the fact that Na-amphibole growth occurred after the development of the eclogitic paragenesis (**11)**

For this sample, the maximum pressure (eclogitic conditions) is estimated at 21 ± 2 kbar (Fig. 5**).(13)**

CUl6: The temperature is poorly constrained **(12)** in this sample as blueschist retrogression is well developed. Nevertheless, thermometry on two garnet – clinopyroxene pairs yields 565 ± 70°C, while the pressure is estimated at 18 ± 1 kbar. **(13)**. The occurrence of secondary glaucophane in equilibrium with paragonite and clinozoïsite roughly limits the temperature field at 550°C for 20 kbar, and 400°C for 5 kbar for the blueschist stage (Maresh, 1977). (Fig. 5) **(11)**

LV 69: In this sample, the eclogitic paragenesis is not in textural equilibrium with glaucophane, suggesting that eclogitic metamorphic temperature was over 550°C (Maresh, 1977). **11)** Garnet-amphibole thermometry was applied, and there conditions were verified (spessartine in garnet <10%, T<850°C). Graham & Powell (1984) however advise that this thermometer is used with caution for eclogitic paragenesis, because the Fe-Mg equilibrium between garnet and amphibole is not always reached in HP rocks.(**14)** The average temperature obtained with the garnet-amphibole thermometer is 570 ± 55°C on ten pairs, that agree within error with the results of the garnet-clinopyroxene thermometer on four pairs (600 ± 70 °C). These temperatures are in good

agreement with those obtained on sample LV66. The pressure is estimated at 19 ± 1 kbar for an average temperature of 590 ± 80°C. (Fig. 5).

Summary of the Escambray metamorphic conditions:

Petrological analysis of the LV69 metabasite indicates a prograde path from epidote-bearing amphibolitic to barroisite-bearing eclogitic conditions. The P-T conditions for the eclogitic peak is estimated at 19 ± 1 kbar and 590 ± 80 °C. A similar path is recorded by the eclogite LV66 (21 ± 2 kbar, 615 ± 80 °C). Both metabasites show evidence of retrogression beginning in the field of the glaucophane bearing-eclogites. The CUl6 metabasite garnet zonation is in accordance with this prograde path. For this sample, peak metamorphic conditions are located in the eclogitic facies (18 ± 1 kbar, 565 ± 70 °C). The retrogressed path is well preserved, showing a cooling under epidote blueschist facies conditions. Therefore these rocks preserve a counter-clockwise path (Fig. 5) which has been previously reported for eclogites from the Franciscan complex (Wakabayashi,1990; Oh and Liou, l990; Krogh and al., 1994) and described by Smith et al. (1999) for blueschists from the Venezuela.

Geochemistry

Eclogites LV66 and CU16 from Loma La Gloria formation

These samples have intermediate concentrations in SiO_2 = 46.3-50.4%, Mg0 = 4-4.8% and K_2O = 0.6-1 %, high in Al_2O_3 = 20.1% and relatively low in TiO_2 ≤1%, (Table 2). REE chondrite - normalised patterns (Sun & Mc Donough, 1989) for eclogites are presented in Fig. 6a.

The REE abundances of LV66 and CU16 are between 10 and 80 higher than chondritic value and are highly enriched in light REE ((La/Yb)n = 4.4-5.3 and (La/Sm)n = 2.2-2.3) (Table 2).

The CU16 and LV66 HP rocks are rich in LILE (K, Rb, Ba and Pb) and slightly depleted in HFSE (Nb and Ti) (see Fig. 6b and Table 2). In a Ba/TiO_2 ratio versus Ba content diagram (Fig. 7a), these samples plot in the calc-alkaline arc field (Sorensen et a1., 1997). In the Pb/Ce ratio versus Pb content diagram (Fig. 7b), samples LV66 and CU16 plot close to the Cretaceous calc-alkaline arc field defined by Kerr et al. (1999). Moreover our trace element data well compare with analyses from Cretaceous calc-alkaline arc of Central Cuba (samples MAT1-4 from Kerr et al.,1999; Blein et al., 2003) (Fig. 6b), and other Cretaceous calc-alkaline rocks around the Caribbean margin (Donnelly et al., 1990; Lebron & Perfit, 1994; Kerr et al., 1999).

These metabasites have relatively low εNdi values (-2.36 and - l .84; Fig. 8 and Table 3). Similar values have been reported for the Cretaceous Cuban island-arc rocks (Blein et al., 2003) and in various areas such as the Sonde arc (Hoogewerff et al., 1996). These low εNdi values can be explained by assimilation of pelagic and/or terrigeneous sediments by magmas formed during the melting of the subducting plate which results in a magmatism of arc affinity (Ben Othman et al., 1989; Hoogewerff et al., 1996). The participation of such sedimentary component is also well evidenced in the Pb/Ce ratio versus Pb content diagram (Fig. 7b).

Eclogite LV69:

LV69 possess intermediate concentration in SiO_2 (47.2%) and MgO (9.3%), a high Al_2O_3 (l4.8%) and TiO_2 (l.6%) and a low K_2O content (0.2%) (Table 2). It shows a REE chondrite-normalised pattern characterized by a subtle but distinctive light REE depletion (La/Yb)n = 0.8 ; (La/Sm)n = 0.7) typical of the N-MORB type rocks (Table 2 and Fig. 6a), and enrichment in

LILE elements (Rb, Ba and Sr) and U and Pb compared to typical MORB. Sorensen et al. (l997) described similar enrichments for eclogitic rocks associated with MORB type protoliths. These authors suggest the importance of the phengitic component to explain such enrichment. In the Ba/TiO_2 ratio versus Ba content diagram (Fig. 7a) the eclogite LV69 plots on a mixing curve between a phengitic and a MORB end-member. The phengitic contribution could be estimated at around l% (Sorensen et al., l997). The Pb concentration is also controled by the phengitic component as Pb substitutes for K in phengites (Becker et al., 2000). This phengitic contribution could result from a late metasomatism at depth or from hydrothermal alteration of the oceanic floor before subduction (Sorensen et al., l997). The petrological analysis does not show any evidence of a secondary crystallisation of phengite during a metasomatic event as demonstrated in the previous section. We thus favour the pre-metamorphic hydrothermal alteration hypothesis. Moreover the positive anomalies in U and Pb compared to MORB (Sun & Mc Donough, l989) can be explained by an early alteration of the oceanic seafloor. LV69 falls in the field of altered MORB defined by Becker et al. (2000) where Pb and U are added to oceanic basalts during hydrothermal alteration of pelagic sediments and MORB (German et al., l995; Becker et al., 2000). Addition of Pb to a MORB protolith originating from pelagic sediments is well demonstrated on a Pb/Ce ratio versus Pb content diagram (Fig. 7b) where LV69 plots between the MORB end member (Sun & Mc Donough, l989) and the pelagic sediment domain.

LV69 eclogite yields an εNdi ratio of +9.16 (Fig. 8, Table 3), in the typical range of MORB. Its high $(^{87}Sr/^{86}Sr)_i$ initial value (0.70569) (Table 3) points to a seawater hydrothermal component. Since$(^{87}Sr/^{86}Sr)_i$ value for the whole rock, pyroxenes and amphiboles have identical $(^{87}Sr/^{86}Sr)_i$ ratio in LV69, an early alteration of the protolith prior to subduction is likely.

Geochronology

Rb/Sr dating results:

Isochron ages, 65.2 ± 6.6 Ma for LV69 and 67 ± 38 Ma for LV66 (Fig. 19a-b and Table 3), calculated with whole-rock, phengite, garnet, omphacite and amphibole experimental points, have large MSWD values (110 and 381 respectively). The scattering of the experimental points in the isochron digrams and particularly the garnet points which plot significantly above the isochron, are responsible for these high MSWD values. The presence of clinozoïsite inclusions in garnet can be invoked to explain the location of garnet points in the diagrams. Indeed, clinozoïsite has higher levels of Sr compared to Rb (Rb/Sr ≈ 0.0001), whereas the garnet Rb/Sr ratio is around 0.1. Therefore, a small amount of clinozoïsite in garnet can completely alter the $^{87}Rb/^{86}Sr$ garnet ratio. In this case we find Rb/Sr ratios of 0.05 and 0.07 for LV69 and LV66 garnets that are tentatively interpreted as reflecting clinozoïsite inclusions. Accordingly, the garnet points have been removed from age calculation. The four remaining points define an isochron age of 65.9 ± 4.2 Ma (MSWD = 8.4) for LV69 and 69.2 ± 6.9 Ma (MSWD = 15) for LV66, with a $^{87}Sr/^{86}Sr$ initial ratio of 0.7057 ± 0.0001 for LV69 and 0.7055 ± 0.0001 for LV66 (Fig. 9a-b).

Ar/Ar dating: results

Eclogite LV69:

Step heating laser probe analysis of single phengite and barroisite grains gives plateau ages of 69.3 ± 0.6 Ma for 95.5% (Table 4a and Fig. 10a) of the argon released and 69.1 ± 1.3 for 93% (Table 4b and Fig. 10b) of the argon released, respectively. For each sample, the first heating steps contain a large amount of atmospheric argon probably released from the surface and structural defects of the mineral at the beginning of degassing. The $^{37}Ar_{Ca}/^{39}Ar_K$ ratio of barroisite

is constant and close to 15. The corresponding isochron ages are similar to the plateau ages for initial $^{40}Ar/^{36}Ar$ ratios slightly below the atmospheric ratio of 295.5.

Eclogite LV66:

Step-heating laser probe analysis of a single phengite grain gives a plateau age of 68.2 ± 0.6 Ma for 99.5% of the argon released, (Table 4c and Fig. 10c) and a similar isochron age. Spot fusion analyses on a second grain give ages between 66.6 and 72.2 Ma, which is consistent with the step-heating age (Fig. 10f and Table 4d).

Eclogite CU16:

Step-heating laser probe analysis of a phengite grain gives a plateau age of 71 ± 0.7 Ma for 99.2% of argon released (Fig. 10d and Table 4e) which is consistent with the isochron age of 69.8 ± 0.8 Ma. A paragonite grain from the same sample has been analysed and was degassed in essentially two steps because of its low K concentration. Nevertheless, the total gas age of this mica (68.9 ± 0.7 Ma) is compatible with the previous results (Fig. 10e and Table 4f).

Age interpretation:

Since the pioneering work of Dodson (1973), geochronological data have been widely used to constrain the cooling history of rocks. Closure temperature for white mica ranges from 350 to 450°C for the Ar/Ar system (Purdy and Jäger, 1976; Blankenburg et al., 1989; Kirschner et al., 1996) and from 500 to 550°C for the Rb/Sr system (Purdy and Jäger, 1976; Blankenburg et al., 1989). Closure temperature for the Ar/Ar system in barroisite is expected to be between 550 and 650°C (Dahl, 1996a; Villa et al., 1998). It has been demonstrated that a wide number of parameter can affect the diffusion kinetic of the system (i.e.; pressure, fluids, chemical

composition, deformation, rock's mode…) (Harrison et al., 1985; Monié, 1985; Scaillet et al., 1992; Baker, 1993; Chen et al., 1995 ; Jenkin et al., 1995 ; Dahl, 1996b, Lister & Baldwin, 1996 ; Agard et al., 2002). Since, no consensus exists on the way to interpret geochronological data (as cooling age or crystallisation ages), especially for phengite. Recent $^{40}Ar/^{39}Ar$ work on various generations of phengite from the French Alps demonstrate that ages obtained in this study should be interpreted as crystallisation ages in respect of the metamorphical history (Agard et al., 2002). Taking this into account, we would not discussed our geochronological data in terms of cooling ages, but as crystallisation ages. Previous geochronological work on the Escambray massif gave ages between 68 and 85 Ma using K-Ar dating on white micas (Somin and Millan, l981; Millan and Somin, 1985; Hatten et al., 1988; Iturralde-Vinent et al., 1996) that were interpreted as exhumation ages. The scatter of ages probably results from combined effects of argon loss, excess argon or complex mineralogy. We consider the Ar/Ar and Rb/Sr ages of 66 to 70 Ma as corresponding to the minimum age for the eclogitisation of samples LV66, LV69 and CU16 as dating were carried on eclogitic minerals (except for CU16 paragonite). Moreover if the protolith for samples LV66 and CU16 is the Cretaceous calc-alkaline arc, the age of the HP metamorphism must be less than 85-110 Ma.

Geodynamic implications and discussion:

The cold retrogressed P-T path observed for the Escambray eclogites is characteristic of rock exhumation during an active subduction (Ernst, 1988; Schwartz et al., 2000). A continuous burying of cold oceanic crust will maintain a cold thermal gradient (thermal depression) in the area of the rock exhumation and thus could result in a cold retrogressed path (Ernst, 1988; Krogh & Liou, 1994). Several models invoking initiation of a new subduction have been proposed to

explain counter-clockwise P-T paths observed in some eclogites (Cloos, 1985; Peacock, 1987; Wakabayashi, 1990, 1992; Krogh et al., 1994; Encarnación et al., 1995). In this case, during the early stages of the subduction, the hanging wall will cool progressively with a decrease of the thermal gradient between the time of burial and that of exhumation. Smith et al. (1999) adapted this model to the subduction reversal occurring in the late Cretaceous in the Caribbean to explain the counter-clockwise PT path recorded in Venezuela. However, no evidence of a subduction reversal has been found in Cuba.

The geochemical study demonstrates that protoliths of the LV66 and CU16 eclogites exhibit geochemical characteristics similar to those of the Cretaceous calc-alkaline arc (Donnelly et al., 1990; Lebron & Perfit, 1994; Kerr et al., 1999). As Loma La Gloria formation is a metasedimentary unit of Jurassic age (Millan, 1997a), the eclogites intercalated within cannot be coherent with this formation if they are interpreted as fragments of the Cretaceous calc-alkaline arc. We propose that slices of the Cretaceous arc were tectonically intercalated with sediments as the subduction was still active. If eclogites CU16 and LV66 derived from the Cretaceous calc-alkaline arc, another model can be proposed to explain the metamorphic history of these samples. The collision between the Early Cretaceous island arc and the Yucatan peninsula may have caused several perturbations in the subduction regime. The decrease of the subduction velocity due to the collision around the Cenomanian is thought to induce an increase of the thermal gradient in the slab area related to a slab retreat (Papier des Japonais). New activation of the subduction and the cooling of the hanging wall at the end of the arc activity will induce a decrease of the thermal gradient after Cenomanian. In this model, rocks subducted around Cenomanian time will record a warmer path during their burial than during their exhumation. If the protolith of samples CU16 and LV66 is the calc-alkaline island arc, burial has necessarily occurred after Albian. More precisely, incorporation of some arc fragments to the subduction

trench should be contemporaneous with the Cenomanian collision. This temporal constraint is consistent with the model proposed above.

For the Escambray HP terranes, the exhumation of the subducted plate and arc fragments would occur in a context of active subduction. The vergence of the syn-eclogitic thrusts (top towards the SW) is compatible with the occurrence of a NE-dipping subdction zone during the Upper Cretaceous. In this model, unit III of the Escambray massif would correspond to a slice of the Pacific plate; LV69 representing the oceanic crust and CU16 and LV66 arc fragments intercalated with oceanic sediments. Since this model has been formulated on the basis of the study of only three samples from the Escambray massif, it is not possible to extend our interpretation to the whole Escambray massif. Nevertheless this study shows that an extended work on the eclogitic protoliths of the Escambray massif should permit a more precise understanding of its history.

Independent of this model, a general exhumation mechanism can be discussed. According to a corner flow mechanism (Cloos, 1982; Allemand & Lardeaux, 1997; Guillot et al., 2001; Schwartz et al., 2001), materials trapped between the slab and the hanging wall will rise up to the surface in a viscous return flow due to the dynamics of subduction. This mechanism is generally invoked to explain the occurrence of high-grade tectonic blocks in a mud-matrix melange (Platt, 1993). However, the Escambray massif does not correspond to a melange zone in the sense of Cloos (1982) or Schwartz et al. (2000) for which each eclogitic block embedded in a metasedimentary or serpentinite matrix records specific P-T conditions. In fact, the studied samples record similar P-T evolution suggesting that they belong to the same tectono-metamorphic slice (unit III). Moreover, previous studies by Millan and Somin (1981) and Grevel (2000) clearly show that unit III is thrust over less metamorphosed tectono-metamorphic units. **(23)** This situation is very similar to that described in Hispaniola by Mann and Gordon (1996)

and Goncalvez et al., (2000) involving the underplating of metasedimentary and magmatic materials (basalts + serpentines) coming from the upper part of the subducted oceanic crust or from the island arc.

It is noticeable that the exhumation of HP/LT rocks from the Sancti Spiritus dome occurred at around 70 Ma which corresponds to the beginning of the collision between the Bahamas platform and the Cretaceous island arc. Even if the exhumation is synchronous with the northeastward subduction of the Farallon plate, the exhumation started with a main collisional event North of the Island arc. This observation shows that several changes in the subduction kinematics due to a collision forward should set off the exhumation of HP fragments from the slab as suggested by Ernst and Liou (1999) for the exhumation of UHP rocks.

Precise dating of the burial would be interesting to calculate the burial rate and to estimate subduction velocity. Geochronological systems used in this study do not allow to calculate cooling rate and exhumation velocity. Calculating all these parameters should permit numerical modelling of the thermal evolution in a dynamic wedge as a function of the subduction velocity and test the model proposed above for the anticlockwise PT path.

Conclusions:

1) The geochemical signatures of the eclogites LV69, LV66 and CU16 suggest that LV69 derived from a N-MORB type protolith which is likely to be Pacific oceanic crust, and that both samples LV66 and CU16 from Loma La Gloria formation derived from a calc-alkaline arc which can be correlated with fragments of the Cretaceous calc-alkaline arc tectonically imbricated with Jurassic sediments.

2) The metamorphic study of the Escambray eclogites and blueschists reveales that these rocks followed a cold thermal gradient during their exhumation. This retrogressed trajectory is characteristic of an exhumation during an active subduction.

3) Geochronological Ar/Ar and Rb/Sr data suggest a rapid exhumation stage at about 70 Ma. This stage can be correlated with the beginning of the collision between the Cretaceous island arc and the Bahamas platform.

4) All these data show that the exhumation of the HP/LT rocks from the Escambray massif occurred during a period of active subduction. The exhumation of some metamorphosed slab fragments should be set off by the collisional events in front of the subduction plate and should occur in a context of accretionary wedge by underplating of oceanic and arc-related materials.

Acknowlegments:

We thank Paddy O'Brien for providing us the garnet-omphacite-phengite program. This study was supported by a CNRS-INSU "Intérieure de la Terre" grant.

References:

Agard, P., Monié, P., Jolivet, L. & Goffé, B., 2002. Exhumation of the Schistes Lustrés complex : *in situ* laser probe $^{40}Ar/^{39}Ar$ constraints and implications for the western Alps. *Journal of Metamorphic Geology*, **20**, 599-618.

Ahnert, F., 1970. Functional relationships between denudation, relief, and upflit in large mid-latitude drainage basins. *American Journal of Science*, **268**, 243-263.

Allemand, P. & Lardeaux, J.M., 1997. Strain partitioning and metamorphism in a deformable orogenic wedge: Application to the Alpine belt. *Tectonophysics*, **280**, 157-169.

Baker, D.R., 1993. Measurement of diffusion at high temperatures and pressures in silicate systems. In: *Short Course Handbook on Experiments at High Pressures and Applications to the Earth's Mantel. Short course handbook* (ed. Luth, R.W.), **21**, 305-355.

Becker, H., Jochum, K.P. & Carlson, R.W., 2000. Trace element fraction during dehydration of eclogites from high-pressure terranes and the implications for element fluxes in subduction zones. *Chemical Geology*, **163**, 65-99.

Ben Othman, D., White, W.M. & Patchett, J., 1989. The geochemistry of marine sediments, island arc magma genesis and crust-mantle recycling. *Earth and Planetery Science Letters*, **94**, 1-21.

Birck, J.L. & Allègre, C.J., 1978. Chronology and chemical history of the parent body of basaltic achondrites studied by the $^{87}Sr/^{86}Sr$ method. *Earth and Planetery Science Letters*, **39**, 37-51.

Blankenburg, F.V., Villa, I.M., Baur, H., Morteani, G. & Steiger, R.H., 1989. Time calibration of a PT-path from the western Tauern Window, Eastern Alps: the problem of closure temperatures. *Contributions to Mineralogy and Petrology*, **101**, 1-11.

Blein O., Guillot S., Lapierre H., Mercier de Lepinay, B., Lardeaux J.M., Millan Trujillo G.M., Campos M., Garcia A. (2003) - Geochemistry of the Mabujina complex, Central Cuba: Implications on the Cuban Cretaceous arc-rocks. **Journal of Geology**,111, 00-00.i n press.

Bousquet, R., Goffé, B., Henry, P., Pichon, X.L. & Chopin, C., 1997. Kinematic, thermal and petrological model of the Central Alps; Lepontine metamorphism in the upper crust and eclogitisation of the lower crust. *Tectonophysics*, **273**, 105-127.

Bralower, T.J. & Iturralde-Vinent, M.A., 1997. Micropaleontological dating of the collision between the North American plate and the Greater Antilles arc in western Cuba. *Palaios*, **12**, 133-150.

Burke, K., 1988. Tectonic evolution of the Caribbean. *Annual Reviews of Earth and Planetary Science*, **16**, 201-230.

Carswell, D.A., O'Brien, P.J., Wilson, R.N. & Zhai, M., 1997. Thermobarometry of phengite-bearing eclogites in the Dabie Mountains of central China. *Journal of Metamorphic Geology*, **15**, 239-252.

Chemenda, A.I., Mattauer, M., Malavieille, J. & Bokun, A.N., 1995. A mechanism for syncollisional rock exhumation and associated normal faulting. *Earth and Planetery Science Letters* , **132**, 225-232.

Chen, D., Jia, M., Li, O., Lu, Q., Xie, H. & Hou, W., 1995. Argon diffusion from biotite at high temperature and pressure. *Science in China*, **Serie B 38**, 221-227.

Cloos, M., 1985. Thermal evolution of convergent plate margins: thermal modeling and reevaluation of isotopic Ar-ages for blueschists in the Franciscan complex of California. *Tectonics*, **4**, 421-433.

Cloos, M., 1982. Flow melanges: numerical modelling and geologic constraints on their origin in the Franciscan sudbuction complex, California. *Geological Society of America Bulletin*, **93**, 330-345.

Crank, J., 1975. *The mathematics of diffusion*, 2nd edition. *Caledon*, Oxford.

Dahl, P.S., 1996a. The effects of composition on retentivity of Ar and O in hornblende and empirical related amphiboles: a field tested empirical model. *Geochimica et Cosmochimica Acta*, **60**, 3687-3700.

Dahl, P.S., 1996b. The crystal-chemical basis for Ar retention in micas: inferences from interlayer partitioning and implications for geochronology. *Contributions to Mineralogy and Petrology*, **123**, 335-374.

Dalrymple, G.B., 1989. The GLM continuous laser system for $^{40}Ar/^{39}Ar$ dating : description and performance characteristics. In : *New frontiers in Stable Isotopic Research : Laser Probes,*

Ion Probes and Small-Samples Analysis (Shanks, W.C. & Criss, R.E. eds). *U.S.G.S. Bulletin*, **1890**, 89-86.

Davies, J.H. & Von Blanckenburg, F., 1995. Slab breakoff: a model of lithospheric detachment and its test in the magmatism and deformation of collisional orogens. *Earth and Planetery Science Letters*, **129**, 85-102.

Dodson, M.H., 1973. Closure temperature in cooling geochronological and petrological systems. *Contributions to Mineralogy and Petrology*, **40**, 259-274.

Dolan, J., Mann, P., De Zoeten, R., Heubeck, C., Shiroma, J. & Monechi, S., 1991. Sedimentologic, stratigraphic and tectonic synthesis of Eocene-Miocene sedimentary basins, Hispaniola and Puerto-Rico. In: *Geologic and tectonic developement of the North America-Caribbean Plate Boundary in Hispaniola* (eds Mann, P., Draper, G. & Lewis, J.F.) pp 217-264. *Special paper – Geological Society of America,* **262**, 217-263.

Donnelly, T., Beets, D., Carr, M., Jackso et al., 1990. History and tectonic setting of Caribbean magmatism. In: The Caribbean region: Boulder, Colorado, (eds. Dengo G. & Case J.E.), *Special paper- Geological Society of America,* The Geology of North America, **H**, 339-374.

Ellis, D.J. & Green, D.H., 1979. An experimental study of the effect of Ca upon garnet-clinopyroxene Fe-Mg exchange equilibria. *Contributions to Mineralogy and Petrology*, **71**, 13-22.

Encarnación, J.P., Essene, E.J., Makasa, S.B. & Hall, C.H., 1995. High pressure and temperature subophiolitic kyanite-garnet amphibolites generated during initiation of mid Tertiary subduction, Palawan, Philippines. *Journal of Petrology*, **36**, 1481-1503.

England, P.C. & Holland, T.J.B., 1979. Archimedes and the tauern eclogites: the role of buoyancy in the preservation of exotic tectonic blocks. *Earth and Planetary Science Letters*, **44**, 287-294.

Ernst, W.G., 1988. Tectonic history of subduction zones inferred from retrogressed blueschist P-T paths. *Geology*, **16**, 1081-1084.

Ernst, W. G. & Liou, J. G., 1999. Overview of UHP metamorphism and tectonics in well studied collisional orogens. *International Geology Review*, **41**, 477-493.

García-Casco, A., Torres-Roldán, R.L., Millán, G., Monié P. & Schneider, J., 2002. Oscillatory zoning in eclogitic garnet and amphibole, northern serpentinite melange, Cuba: A record of tectonic instability during subduction? *Journal of Metamorphic Geology*, **20**, 1-18.

Garcia-Casco, A., Torres-Roldán, R. L., Millán, G., Monié, P. & Haissen, F. , 2001. High-grade metamorphism and hydrous melting of metapelites in the Pinos terrane (W Cuba): Evidence for crustal thickening and extension in the northern Caribbean collisional belt. *Journal of Metamorphic Geology*, 2001, **19**, 699-715.

German, C.R., Barreiro, B.A., Higgs, N.C., Nelson, T.A., Ludford, E.M. & Palmer, M.R., 1995. Seawater-metasomatism in hydrothermal sediments (Escanaba Trough, northest Pacific). *Chemical Geology*, **119**, 175-190.

Gonçalves, P., Guillot, S., Lardeaux, J.M., Nicollet, C. & Mercier de Lepinay, B., 2000. Thrusting and sinistrial wrenching in a pre-Eocene HP-LT Caribbean accretionary wedge (Samana Peninsula, Dominican Pepublic). *Geodinamica Acta*, **13**, 119-132.

Gordon, M.B., Mann, P., Cáceres, D. & Flores, R., 1997. Cenozoic tectonic history of the North America-Caribbean plate boundary zone in western Cuba. *Journal of Geophysical Research*, **102**, 10055-10082.

Grafe, F., Stanek, K.P., Baumann, A., Maresch, W.V., Hames, W.E., Grevel, C. & Millan, G., 2001. Rb-Sr and $^{40}Ar/^{39}Ar$ mineral ages of granitoid intrusives in the Mabujina Unit, Central Cuba: thermal exhumation history of the Escambray massif. *Journal of Geology*, **109**, 615-631.

Graham, C.M. & Powell, R., 1984. A garnet-hornblende geothermometer: calibration, testing, and application to the Pelona schist, Southwern California. *Journal of Metamorphic Geology*, **2**, 13-31.

Grevel, C., 2000. Druck- und temperaturentwicklung der metamorphen deckeneinheiten des Escambray massives, Kuba (Pressure and temperature history of the metamorphic nappes of the Escambray massif, Cuba). *PhD Thesis, Ruhr-Universität Bochum, Bochum*.

Guillot, S., Hattori, K. H., De Sigoyer, J., Naegler, T. & Auzende, A.L., 2001. Evidence of hydration of the mantle wedge and its role in the exhumation of eclogites. *Earth and Planetery Science Letters*, **193**, 115-127.

Harrison, T.M., Duncan, I. & MacDougall, I., 1985. Diffusion of ^{40}Ar in biotite: Temperature, pressure and compositional effects. *Geochimica et Cosmochimica Acta*, **49**, 2461-2468.

Hatten et al., 1989. Rocas metamorficas de alta presion. In : *Cuba: nuevos datos acerca sus edades. Resumenes del Primer Congreso Cubano de Geologia*, 118-119.

Hatten, C.W., Somin, M.L., Millan, G., Renne, P., Kistler, R.V. & Mattison, J.M., 1988. Tectonostratigraphic units of Central Cuba. *Memorias de la Oncena Conferencias Geological del Caribe, Barbos*, **35**, 1-13.

Hodges, K.V. & Spear, F.S., 1982. Geothermometry, geobarometry and the Al_2SiO_5 triple point at Mt. Moosilauke, New Hampshire. *American Mineralogist*, **67**, 1118-1134.

Holland, T.J.B., 1980. The reaction albite = jadeite + quartz determined experimentally in the range 600-1200°C. *American Mineralogist*, **65**, 129-134.

Holland, T.J.B. & Powell, R., 1990. An enlarged and updated internally consistent thermodynamic dataset with uncertainties and correlations : the system K_2O-Na_2O-CaO-MgO-MnO-FeO-Fe_2O_3-Al_2O_3-TiO_2-SiO_2-C-H_2-O_2. *Journal of Metamorphic Geology*, **8**, 89-124.

Holland, T.J.B. & Powell, R., 1985. An internally consistent thermodynamic dataset with uncertainties and correlations : 2. Data and results. *Journal of Metamorphic Geology*, **3**, 327-342.

Hoogewerff, J.A., Van Bergen, M.J., Vroon, P.Z. et al., 1996. U-series, Sr-Nd-Pb isotopes and trace element systematics accross an active island arc-continent collision zone: implications for element transfert at the slab-wedge interface. *Geochimica et Cosmochimica Acta*, **61**,1057-1072.

Huston, F., Mann, P. & Renne, P., 1998. $^{40}Ar/^{39}Ar$ dating of single muscovite grains in Jurassic siliclastic rocks (San Cayentano Formation): Constraints on the paleoposition of western Cuba. *Geology*, **26**, 83-86.

Iturralde-Vinent, M.A., 1997. Introduccion a la geologia de Cuba. In: *Estudios sobre geologia de Cuba*, (eds Furrazola-Bernudez, G.F. and Nunez-Cambra, K.E.) 35-68. *Centro National de Information Geologica, La Habana, Cuba.*

Iturralde-Vinent, M. A., 1996a. Introduction to Cuban Geology and Geophysics. In: *Ofiolitas y Arcos Volcánicos de Cuba* (ed. Iturralde-Vinent, M. A.). *IGCP Project 364, Special Contribution*, **1**, 3-35.

Iturralde-Vinent, M.A., 1996b. Cuba: El arco de islas volcanicas del Cretacio. In: *Ophiolitas y arcos volcanicos de Cuba* (ed. Iturralde-Vinent, M.A.) *IGCP Project 364, Special Contribution*, 179-189.

Iturralde-Vinent, M.A., 1996c. Estratigrafia del arco volcanico Cretacico de Cuba. In: *Ophiolitas y arcos volcanicos de Cuba* (ed. Iturralde-Vinent, M.A.) *IGCP Project 364, Special Contribution*, 190-226.

Iturralde-Vinent, M. A., Millán, G., Korkas, L., Nagy, E. & Pajón, J., 1996. Geological interpretation of the Cuban K-Ar data base. In: *Ofiolitas y Arcos Volcánicos de Cuba* (ed. Iturralde-Vinent, M. A.). *IGCP Project 364, Special Contribution*, **1**, 48-69.

Iturralde-Vinent, M.A., 1994. Cuban geology: A new plate tectonic synthesis. *Journal of Petroleum Geology*, **17**, 39-70.

Jenkin, G. R. T., Rogers, G., Fallick, A. E. & Farrow, C. M., 1995. Rb-Sr closure temperatures in bi-mineralic rocks: a mode effect and test for different diffusion models. *Chemical Geology*, **122**, 227-240.

Kerr, A.C., Iturralde-Vinent, M.A., Saunders, A.D., Babbs, T.L. & Tarney, J., 1999. A new plate tectonic model of the Caraibbean: Implications from a geochemical reconnaissance of Cuban Mesozoic volcanic rocks. *Geological Society of America Bullettin*, **111**, 1581-1599.

Kerr, A.C., Marriner, G.F., Tarney, J., Nivia, A., Saunders, A.D., Thirlwall, M.F. & Sinton, C.W., 1997. Cretaceous basaltic terranes in Western Colombia : Elemental, chronological and Sr-Nd isotopic constraints on petrogenesis. *Journal of Petrology*, **38**, 677-702.

Kirschner, D.L., Cosca, M.A., Masson, H. & Hunziker, J.C., 1996. Staircase $^{40}Ar/^{39}Ar$ spectra of fine grained white mica: timing and duration of deformation and empirical constraints on argon diffusion. *Geology*, **24**, 152-168.

Kretz, R., 1983. Symbols for rock-forming minerals. *American Mineralogist*, **68**, 277-279.

Krogh Ravna, E., 2000. The garnet-clinopyroxene Fe^{2+}-Mg geothermometer : an updated calibration. *Journal of Metamorphic Geology*, **18**, 211-219.

Krogh, E.J. & Raheim, A., 1978. Temperature and pressure dependences of Fe-Mg partitioning between garnet and phengite, with particular reference to eclogites. *Contribution to Mineralogy and Petrology*, **66**, 75-80.

Krogh, E.J., Oh, C.W. & Liou, J.G., 1994. Polyphase and anticlockwise P-T evolution for Fransiscan eclogites and blueschists from Jenner, California, USA. *Journal of Metamorphic Geology*, **12**, 121-134.

Leake, B.E., Woolley, A.R., ARPS, C.E.S. et al., 1997. Nomenclature of amphiboles. Report of the subcommittee on amphiboles of the international mineralogical association commission on new minerals and mineral names. *European Journal of Mineralogy*, **9**, 623-651.

Lebron, M.C. & Perfit, M.R., 1994. Petrochemistry and tectonic sgnificance of Cretaceous island arc rocks. Cordillera Central, Dominican Republic. *Tectonophysics*, **229**, 69-100.

Lebron, M.C. & Perfit, M.R., 1993. Stratigraphic and petrochemical dat support subduction polarity reversal of the Cretaceous Caribbean island-arc. *Journal of Geology*, **101**, 389-396.

Lister, G.S. & Baldwin, S.L., 1996. Modelling the effect of arbitrary P-T-t histories on argon diffusion using the MacArgon program for the Apple Macintosch. *Tectonophysics*, **253**, 83-109.

Ludwig, K.R., 1994. ISOPLOT: a plotting and regrssion program for radiogenic-isotope data for IBM-PC compatible computers, version 2.02. *U. S. Geological Survey Open File*, Report No 88-557.

Mann, P. & Gordon, M. B., 1996. Tectonic uplift and exhumation of blueschist belts along transpressional strike-slip fault zones. *Geophysical Monograph*, **96**, 143-154.

Mann, P., Taylor, F.W., Edwards, R.L. & Ku, T.L., 1995. Actively evolving microplaque formation by oblique collision and sideways motion alog strike-slip fault: An example from the Northeastern Caribbean plate margin. *Tectonophysics*, **246**, 1-69.

Maresh, W.V., 1977. Experimental study on Glaucophane, an analysis on present knowledge. *Tectonophysics*, **43**, 109-125.

McDougall, I. & Harrison, T.M., 1988. Geochronology and thermochronology by $^{40}Ar/^{39}Ar$ method. Oxford monographs on geology and geophysics. Oxford University Press.

Millán, G., 1997a. Posición estratigráfica de las metamorfitas cubanas. In: Estudios sobre Geología de Cuba (eds. Furrazola Bermúdez G. F. & Núñez Cambra, K. E.), *Centro Nacional de Información Geológica, La Habana, Cuba*, 251-258.

Millán G., 1997b. Geología del macizo metamórfico del Escambray. In: *Estudios sobre Geología de Cuba* (eds. Furrazola Bermúdez G. F. & Núñez Cambra, K. E.), *Centro Nacional de Información Geológica, La Habana, Cuba*, 271-288.

Millán, G., 1996a. Metamorfitas de la asociación ofiolítica de Cuba. In: *Ofiolitas y Arcos Volcánicos de Cuba* (ed. Iturralde-Vinent, M. A.), *IGCP Project 364 Special Contribution*, **1**, 131-146.

Millán, G., 1996b. Geología del Complejo de Mabujina. In: *Ofiolitas y Arcos Volcánicos de Cuba* (ed. Iturralde-Vinent, M. A.), *IGCP Project 364 Special Contribution*, **1**, 147-153.

Millan, G., 1989. Evolucion de la estructura del macizo de Escambray, sur de Cuba Central. *Primer Congreso Cubano de Geologica, Resumenes y Programa*, 100-101.

Millan, G. & Somin, M.L., 1985. Nuevos aspectos sobre de la estratigrafia del macizo metamorfico de Escambray. In: *Contribucion al conocimento geologico de las metamorficas del Escambray del Purial. I.G.P. reporte de Investigation,* **2**, 1-142.

Millán, G. & Somin, M. L., 1981. Litología, estratigrafía, tectónica y metamorfismo del macizo del Escambray. Editora ACC. *La Habana, Cuba*, 104 p.

Monié, P., 1985. La méthode $^{40}Ar/^{39}Ar$ appliquée au métamorphisme alpin dans le Massif Mont-Rose (Alpes Occidentales). Chronologie détaillée depuis 110 Ma. *Eclogae Geologicae Helvetiae*, **78**, 487-516.

Monié, P., Soliva, J., Brunel, M. & Maluski, H., 1994. Les cisaillement mylonitiques du granite de Millas (Pyrénées, France). Age Crétacé $^{40}Ar/^{39}Ar$ et interprétation tectonique. *Bullettin de la Société Geologique de France*, **165**, 559-571.

Morimoto, N., 1988. Nomenclature of pyroxenes. *Bulletin of Mineralogy*, **111**, 535-550.

O'Brien, P.J., Zotov, N., Law, R., Khan, M.A. & Jan, M.Q., 2001. Himalayan eclogites and implications for India-Asia collision. *Geology*, **29**, 435-438.

Oh, C.W. & Liou, J.G., 1990. Metamorphic evolution of two different eclogites in the Franciscan Complex. *Lithos*, **25**, 41-53.

Peacock, S.M., 1987. Creation and preservation of subduction related inverted metamorphic gradients. *Journal of Geophysical Research*, **92**, 12763-12781.

Perfit, M.R. & Heezen, B.C., 1978. The geology and evolution of the Cayman trench. *Geological Society of America Bulletin*, **89**, 115-1174.

Pindell, J.L., 1993. Determination of Euler pole for relative motion of Caribbean and North American plates using slip vectors of interplate earthquakes. *EOS: Transaction of American Geophysical Union*, **74**, 586.

Platt, J.P., 1993. Exhumation of high-pressure rocks: a review of concept and processes. *Terra Nova*, **5**, 119-133.

Platt, J.P., 1986. Dynamic of orogenic wedges and the uplift of high-pressure metamorphic rocks. *Geological Society of America Bulletin*, **97**, 1037-1053.

Powell, R., 1985. Regression diagnostics and robust regression in geothermometer/ geobarometer calibration: the garnet-clinopyroxene geothermometer revisited. *Journal of Metamorphic Geology*, **3**, 231-243.

Powell, R. & Holland, T.J.B., 1988. An internally consistent thermodynamic dataset with uncertainties and correlations : 3. Applications to geobarometry, worked examples and computer program. *Journal of Metamorphic Geology*, **6**, 173-204.

Powell, R. & Holland, T.J.B., 1985. An internally consistent thermodynamic dataset with uncertainties and correlations : 1. Methods and worked examples. *Journal of Metamorphic Geology*, **3**, 327-342.

Purdy, J.W. & Jäger, E., 1976. K-Ar ages on roch forming minerals from the central Alps. *Memoria Instituto Geologia e Mineralogia, Universita di Padova*, 30.

Samson, S.C., & Alexandre, E.C., 1987. Calibration of the interlaboratory $^{40}Ar/^{39}Ar$ dating standard MMHb-1. *Chemical Geology*, **66**, 27-34.

Scaillet, S., Féraud, G., Ballèvre, M. & Amouric, M., 1992. Mg/Fe and [(Mg/Fe)Si-Al_2] compositional control on argon behaviour in high pressure white micas: a $^{40}Ar/^{39}Ar$ continuous laser probe study from the Dora Maira nappe of the internal western Alps, Italy. *Geochimica et Cosmochimica Acta*, **56**, 2851-2872.

Schwartz S., Allemand P., Guillot S. (2001 Numerical model of the effect of serpentinites on the exhumation of eclogitic rocks : insights from the Monviso ophiolitic massif (Western Alps). **Tectonophysics**, 342, 193-206.

Schwartz, S., Lardeaux, J.M., Guillot, S. & Tricart, P., 2000. Diversité du métamorphisme écologique dans le massif ophiolitique du Monviso (Alpes occidentales, Italie). *Geodinamica Acta*, **13**, 169-188.

Sinton, C.W., Duncan, R.A., Storey, M., Lewis, J. & Estrada, J.J., 1998. An oceanic flood basalt province within the Caribbean plate. *Earth and Planetary Science Letters*, **155**, 221-235.

Smith, C.A., Sisson, V.B., Avé Lallemant, H.G. & Copeland, P., 1999. Two contrasting pressure-temperature-time paths in the Villa de Cura blueschist belt, Venezuela: Possible evidence for Late Cretaceous initiation of subduction in the Caribbean. *Geological Society of America Bulletin*, **11**, 831-848.

Somin, M.L. & Millan, G., 1981. Geologia de los complejos metamorficos de Cuba (in russian). *Moscow (e.d.), Nauka*, p. 219.

Sorensen, S.S., Grossman, J.N. & Perfit, M.R., 1997. Phengite hosted LILE enrichment in eclogite and related rocks: implications for fluid-mediated mass tranfert in subduction zone and arc magma genesis. *Journal of Petrology*, **38**, 3-34.

Sun, S.S. & McDonough, W.F., 1989. Chemical and isotopic systematics of oceanic basalts; implications for mantle composition and processes. *Geological Society Special Publication*, **42**, 313-345.

Villa, I.M., 1998. Isotopic closure. *Terra Nova*, **10**, 42-47.

Wadge, G. & Burke, K., 1983. Neogene Caribbean plate rotation and associated Central American tectonic evolution. *Tectonics*, **2**, 633-643.

Wakabayashi, J., 1990. Counterclockwise P-T-t paths from amphibolites, Franciscan complex, California: relics from the early stages of subduction zone metamorphism. *Journal of Geology*, **98**, 657-680.

Wasserburg, B. J., Jacobsen, S. B., DePaolo, D. J., McCulloch, M. T. & Wen, T., 1981. Precise determination of Sm/Nd ratios, Sm and Nd isotopic abundances in standard solutions. *Geochimica et Cosmochimica Acta*, **45**, 2311-2323.

Waters, D.J. & Martin, H.N., 1993. Geobarometry in phengite-bearing eclogites. *Terra Abstracts*, **5**, 410-411.

York, D., 1969. Least squares fitting of a straight line with correlated errors. *Earth and Planetery Science Letters*, **5**, 320-324.

Zhou, B. & Hensen, B.J.,1995. Inherited Sm-Nd isotope components preserved in monazite inclusions within garnets in leucogneiss from East Antarctica and implications for closure temperature studies. *Chemical Geology*, **121**, 317-326.

Figure caption :

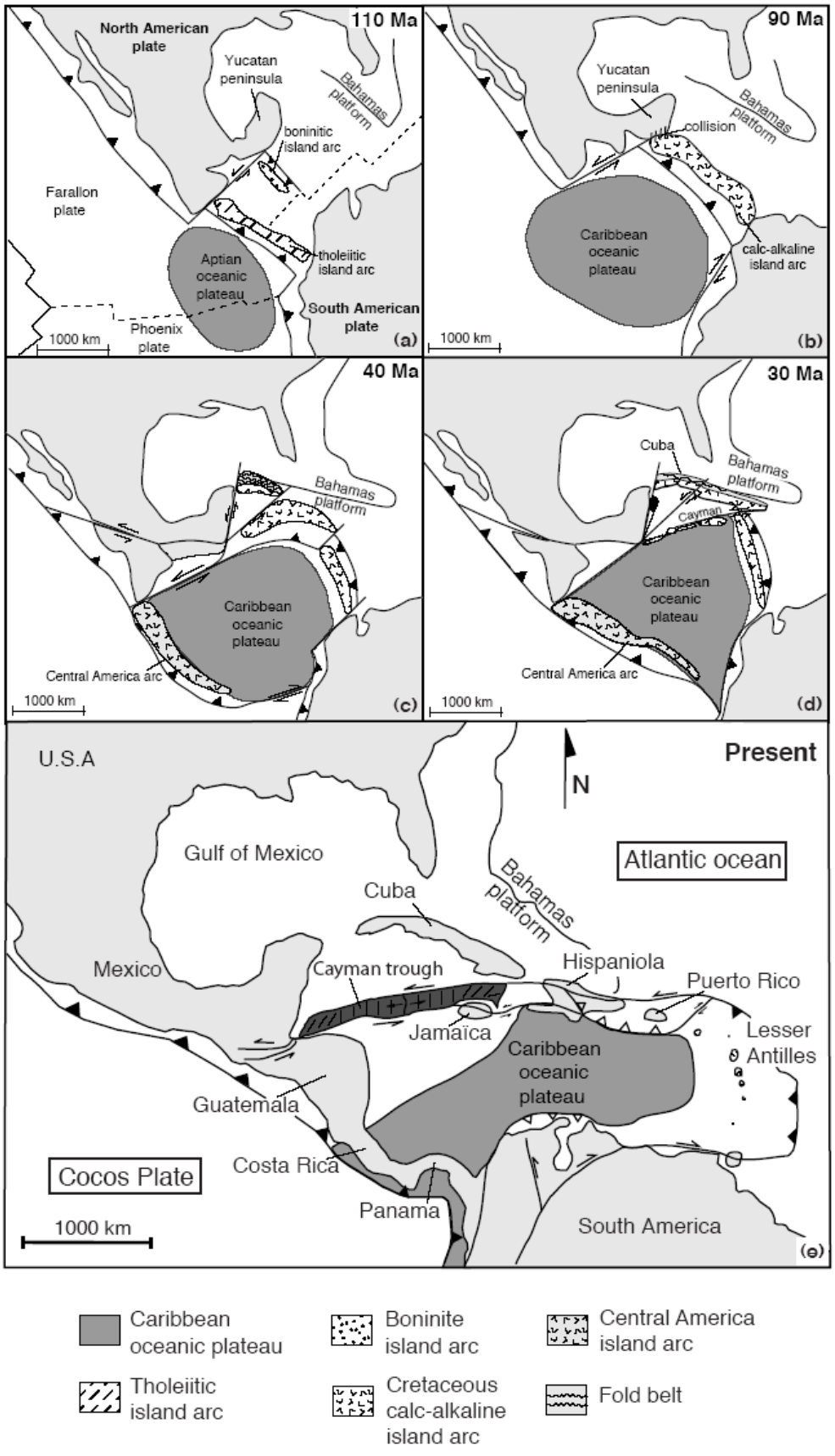
110 Ma
North American plate
Yucatan peninsula
Bahamas platform
boninitic island arc
Farallon plate
Aptian oceanic plateau
tholeiitic island arc
South American plate
Phoenix plate
1000 km
(a)
90 Ma
Yucatan peninsula
Bahamas platform
collision
Caribbean oceanic plateau
calc-alkaline island arc
1000 km
(b)
40 Ma
Bahamas platform
Caribbean oceanic plateau
Central America arc
1000 km
(c)
30 Ma
Cuba
Bahamas platform
Cayman
Caribbean oceanic plateau
Central America arc
1000 km
(d)
Present
U.S.A
N
Gulf of Mexico
Atlantic ocean
Cuba
Bahamas platform
Mexico
Cayman trough
Hispaniola
Puerto Rico
Jamaïca
Lesser Antilles
Caribbean oceanic plateau
Guatemala
Cocos Plate
Costa Rica
Panama
South America
1000 km
(e)
Caribbean oceanic plateau
Boninite island arc
Central America island arc
Tholeiitic island arc
Cretaceous calc-alkaline island arc
Fold belt

Figure 1

Figure 1. (a)-(d) Geodynamical evolution of the Caribbean plate from Cretaceous till Eocene, modified after Huston et al. (1998) and Kerr et al. (1999). (a) Present day map of the Caribbean area after Lebron and Perfit (1991) and Gordon et al. (1997).

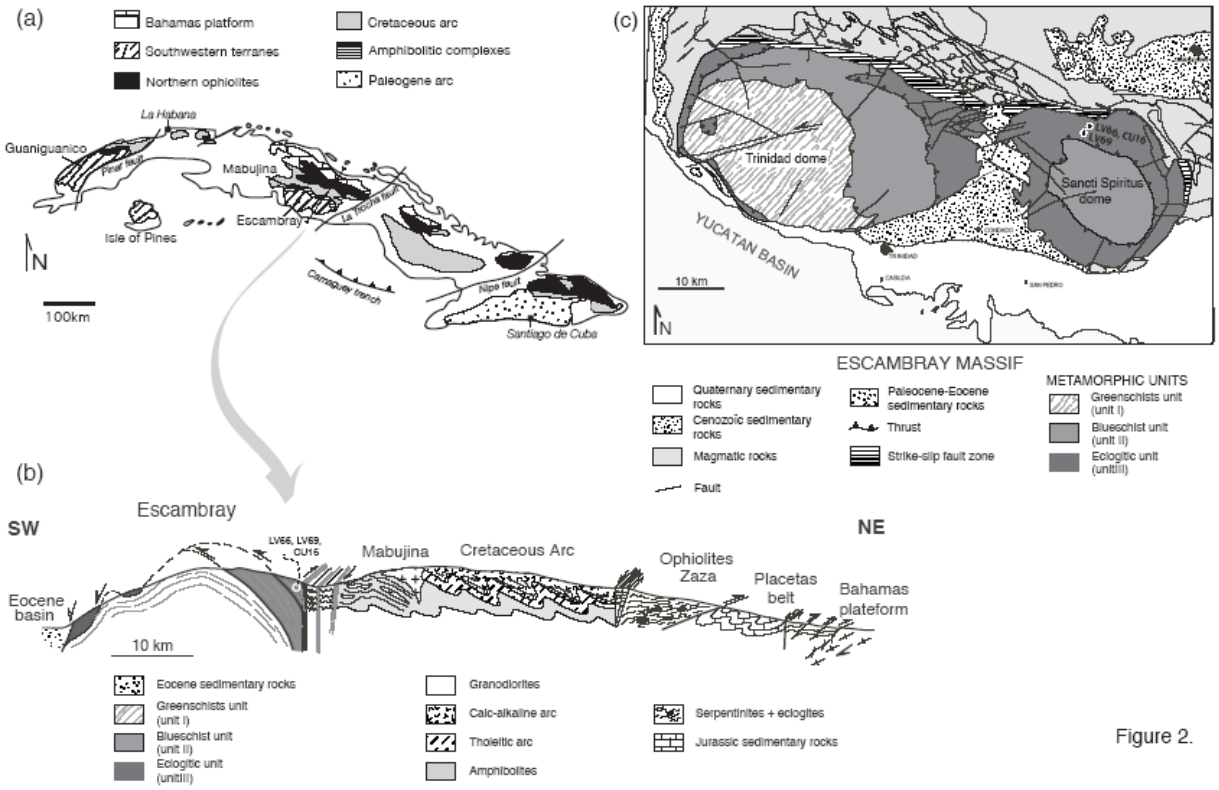

Figure 2.

Figure 2. (a) Geological sketch map of Cuba after Iturralde-Vinent (1996a), the line repport to the cross section (b) and the box show the area of the map (c). (b) Central Cuba schematic cross section with samples location. (c) Geological map of Escambray massif after Millan (1997b) with location of samples LV69, LV66 and CU16.

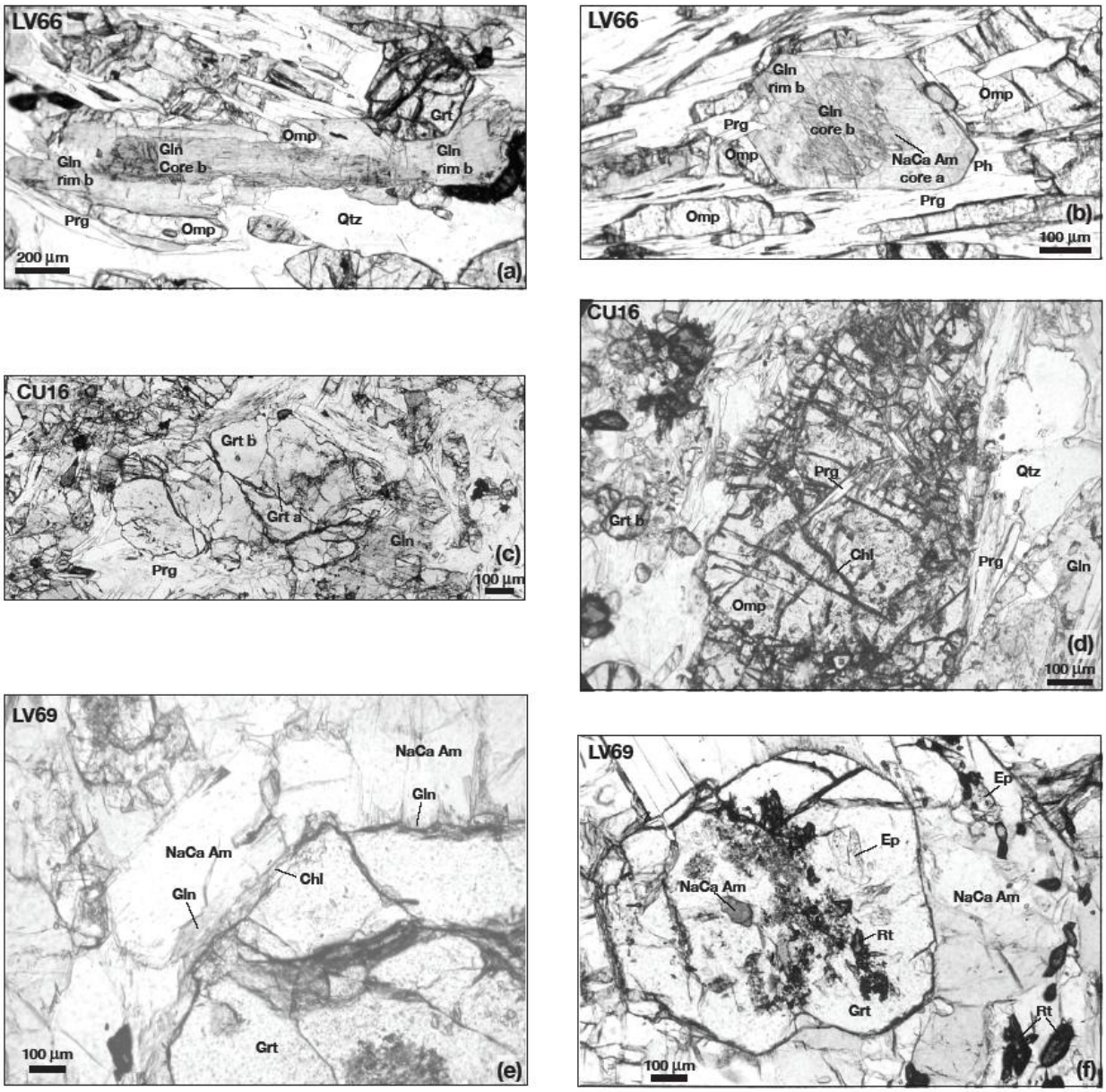

Figure 3.

Figure 3. Photomicrographs of samples (a) LV66, (b) LV69, (c) CU16. gt : garnet ; gln : glaucophane ; pg : paragonite ; prg : pargasite ; ba : barroisite ; omp : omphacite **(26)**

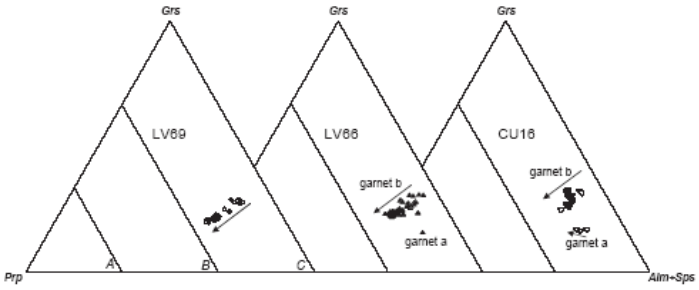

Figure 4.

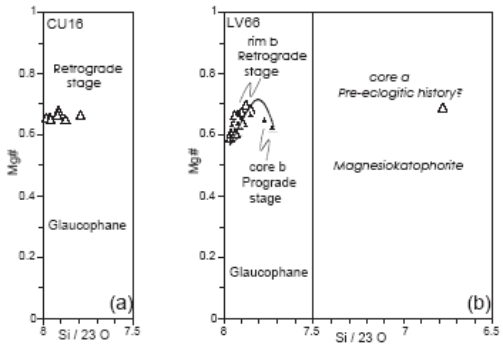

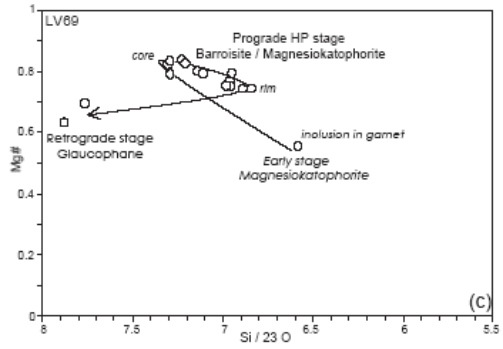

Figure 6.

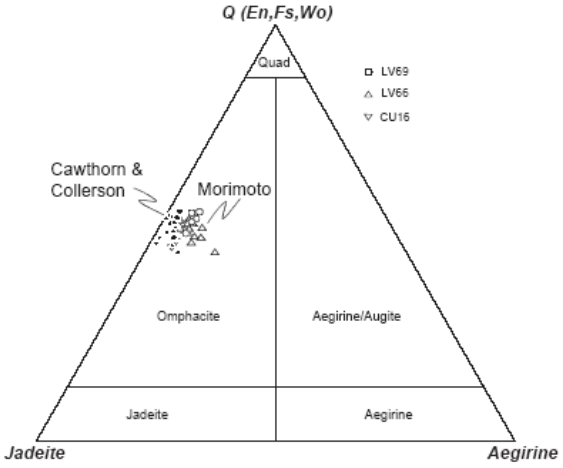

Figure 7.

Figure 4. Zoning pattern of garnets from LV69, CU16 and LV66.

Figure 6. (a) REE normalised patterns of eclogites LV66, LV69 and CU16 normalised to chondrites (Sun & Mc Donough,1989). (b) Traces elements spider diagrams normalised to primitive mantle(Sun & Mc Donough,1989), cretaceous arc fields after Kerr et al. (1999).

Figure 7. (a) Ba/TiO_2 ratio versus Ba content diagram after Sorensen et al. (1997). (b) Pb/Ce ratio versus Pb content diagram. MORB and OIB points after Sun and Mc Donough (1989), cretaceous calc-alkaline field after Kerr et al. (1999).

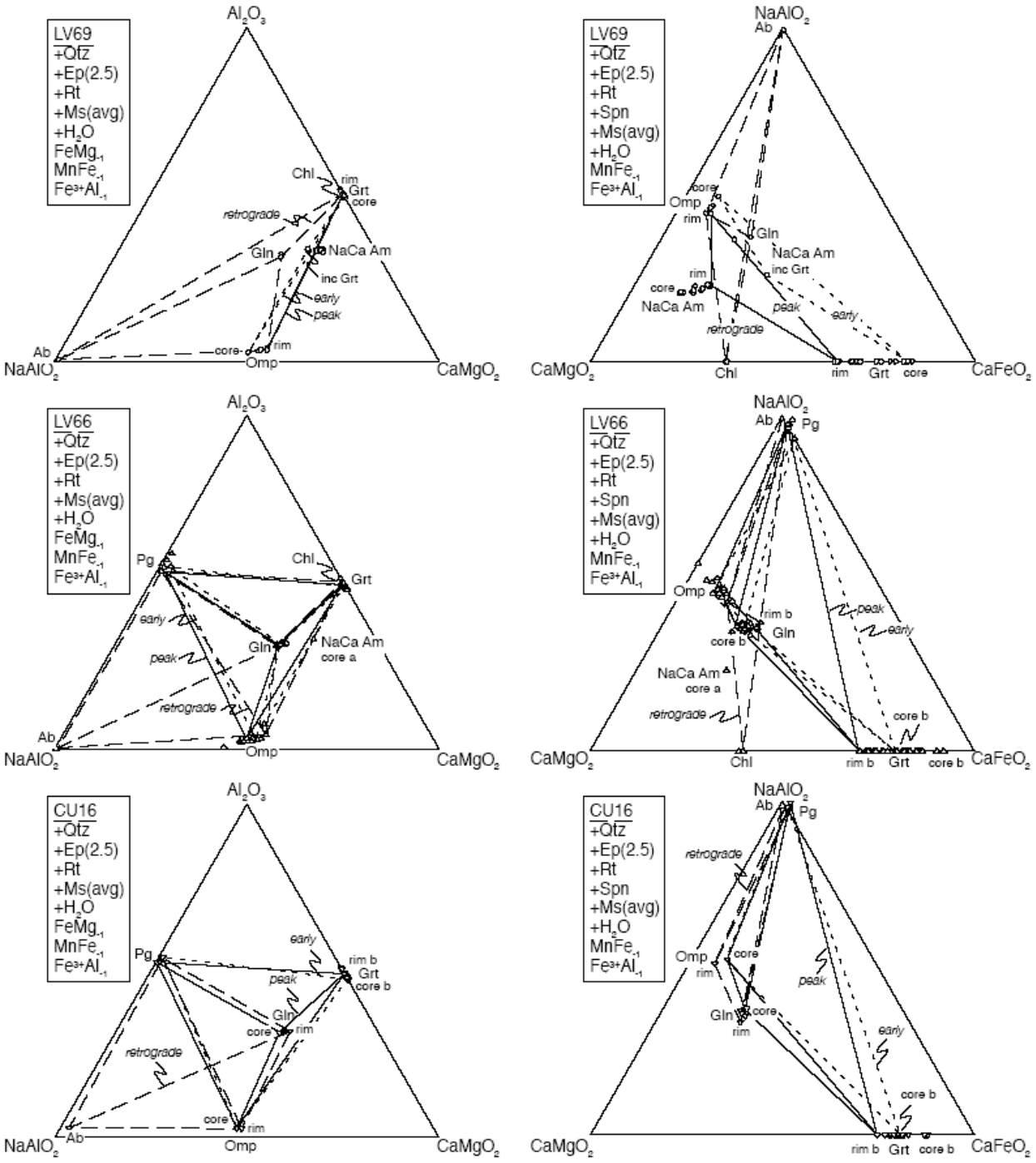

Figure 8.

Figure 8. ($^{87}Sr/^{86}Sr$)i versus εNdi diagram. ($^{143}Nd/^{144}Nd$)i ratios are quoted with εNdi values, calculated with actual ($^{143}Nd/^{144}Nd$)CHUR = 0.512638 (Wasserburg et al., 1981). Initial values are recalculated at 70 Ma.

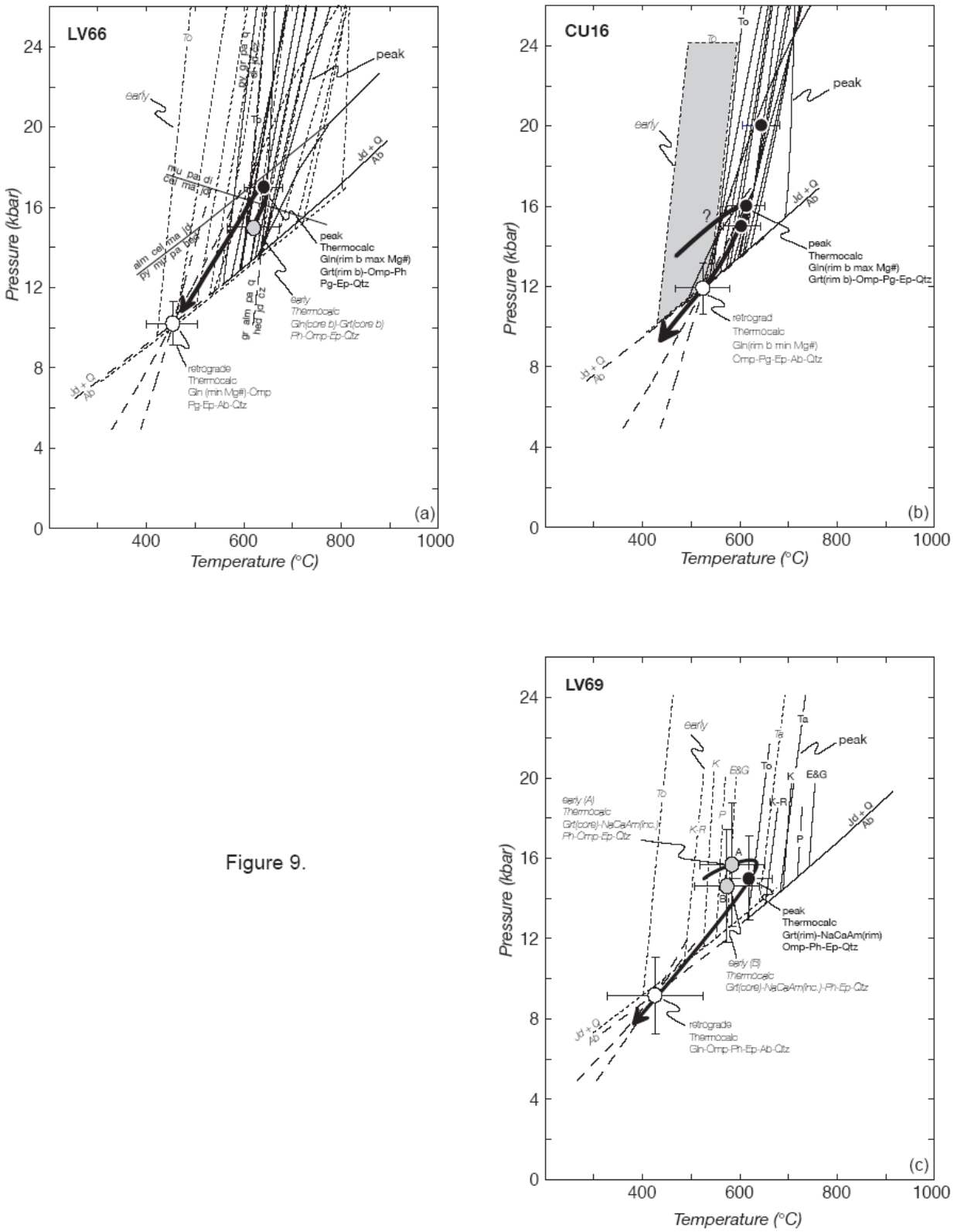

Figure 9.

Figure 9. (a) Eclogite LV69 Rb/Sr isochron. (b) Eclogite LV66 Rb/Sr isochron.

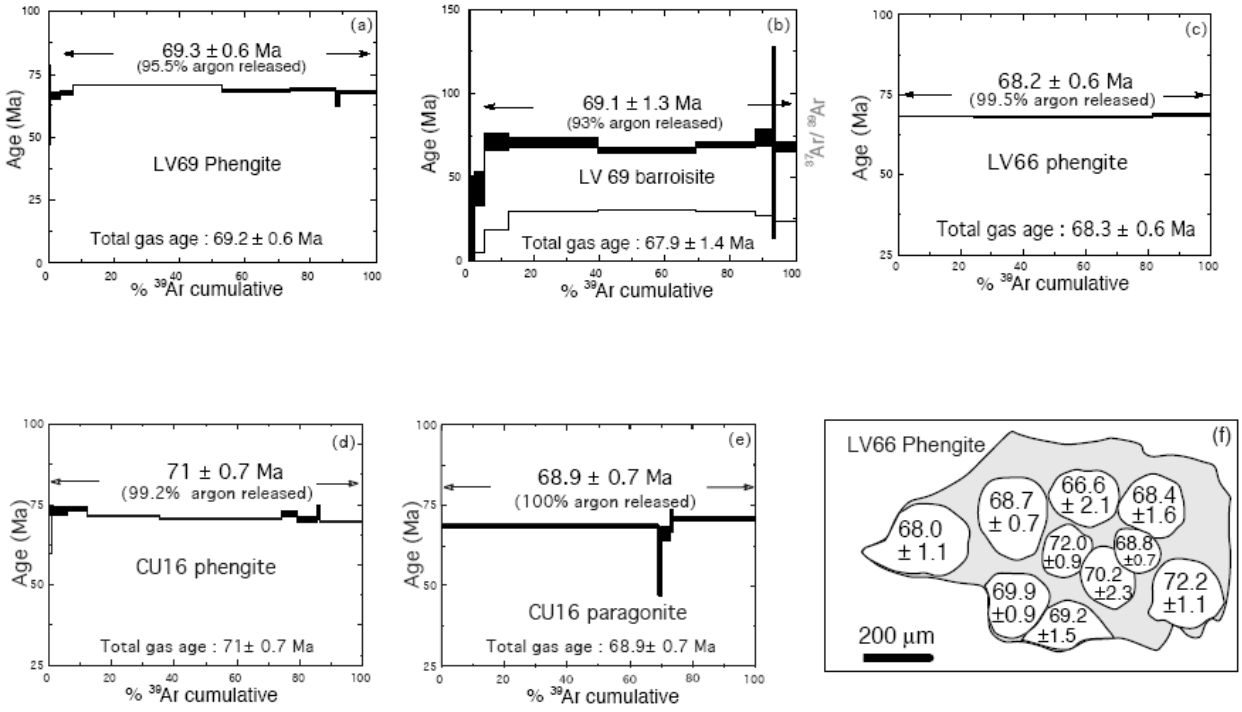
(a)
69.3 ± 0.6 Ma
(95.5% argon released)
LV69 Phengite
Total gas age : 69.2 ± 0.6 Ma
Age (Ma)
% 39Ar cumulative
(b)
69.1 ± 1.3 Ma
(93% argon released)
LV 69 barroisite
Total gas age : 67.9 ± 1.4 Ma
Age (Ma)
% 39Ar cumulative
39Ar/ 39Ar
(c)
68.2 ± 0.6 Ma
(99.5% argon released)
LV66 phengite
Total gas age : 68.3 ± 0.6 Ma
Age (Ma)
% 39Ar cumulative
(d)
71 ± 0.7 Ma
(99.2% argon released)
CU16 phengite
Total gas age : 71± 0.7 Ma
Age (Ma)
% 39Ar cumulative
(e)
68.9 ± 0.7 Ma
(100% argon released)
CU16 paragonite
Total gas age : 68.9± 0.7 Ma
Age (Ma)
% 39Ar cumulative
(f)
LV66 Phengite
68.0 ± 1.1
68.7 ± 0.7
66.6 ± 2.1
68.4 ±1.6
72.0 ±0.9
68.8 ±0.7
70.2 ±2.3
72.2 ±1.1
69.9 ±0.9
69.2 ±1.5
200 μm

Figure 14.